Science of the Total Environment 575 (2017) 767–778

Contents lists available at ScienceDirect

Science of the Total Environment

journal homepage: www.elsevier.com/locate/scitotenv

Investigation of chlorinated solvent pollution with resistivity and induced polarization

Charlotte J. Sparrenbom [a,*], Sofia Åkesson [a], Sara Johansson [b,c], David Hagerberg [a,b], Torleif Dahlin [c]

[a] Department of Geology, Lund University, Sölvegatan 12, SE-223 62 Lund, Sweden
[b] Tyréns AB, Idéon Science Park, Scheelevägen 17, SE-223 70 Lund, Sweden
[c] Engineering Geology, Lund University, Box 118, SE-221 00 Lund, Sweden

HIGHLIGHTS

- Chlorinated solvent pollution has been mapped with geoelectrical (DCIP) methods.
- Geoelectrical (DCIP) measurements are used to map hydrogeological settings.
- Time domain induced polarization show potential for *in situ* remediation monitoring.

GRAPHICAL ABSTRACT

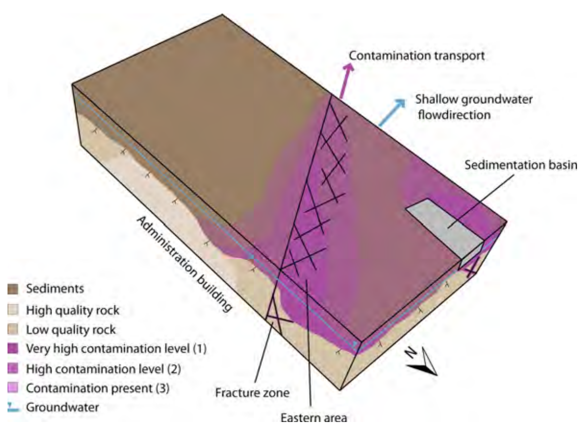

ARTICLE INFO

Article history:
Received 23 June 2016
Received in revised form 14 September 2016
Accepted 15 September 2016
Available online 1 October 2016

Editor: J Jay Gan

Keywords:
DNAPL
Geoelectrical measurements
DCIP
In situ remediation
Hydrogeological setting
Varberg
Sweden

ABSTRACT

Globally, an enormous number of polluted areas are in need of remediation to prevent adverse effects on health and environment. *In situ* remediation and especially the monitoring thereof needs further development to avoid costly and hazardous shipments associated with excavation. The monitoring of *in situ* remediation actions needs easier and cheaper nondestructive methods for evaluation and verification of remediation degree and degradation status of the contaminants. We investigate the Direct Current resistivity and time-domain Induced Polarization tomography (DCIP) method and its use within the context of a DNAPL (Dense Non-Aqueous Phase Liquids) contaminated site in Varberg, Sweden, where an *in situ* remediation pilot test has been performed by stimulated reductive dechlorination by push injection. Our results show that the DCIP technique is an emerging and promising technique for mapping of underground structures and possibly biogeochemical spatial and temporal changes. The methodology could in combination with drilling, sampling and other complementary methods give an almost continuous image of the underground structures and delineation of the pollutant situation. It can be expected to have a future in monitoring approaches measuring time lapse induced polarization (IP), if more research is performed on the parameters and processes affecting the IP-signals verifying the interpretations. The IP technique can possibly be used for verification of the effectiveness of *in situ* remediation actions, as the current sampling methodology is inadequate.

* Corresponding author.
E-mail address: charlotte.sparrenbom@geol.lu.se (C.J. Sparrenbom).

http://dx.doi.org/10.1016/j.scitotenv.2016.09.117
0048-9697/

1. Introduction

In Sweden, >80,000 sites are assumed as or have been identified as contaminated in the national ongoing environmental risk assessment (SEPA, 2014). Presently in Sweden, large numbers of polluted areas are remediated by excavation. The contaminated masses are deposited at landfills, or in best case off-site treatment efforts are applied. *In situ* remediation and especially the monitoring thereof needs further development to avoid the costly and somewhat hazardous shipments associated with excavation. Therefore the recommendation issued by SEPA (2014) is to increase the use of alternative methods *versus* the common "dig and treat" approach. The monitoring of *in situ* remediation actions needs easier and cheaper nondestructive methods for evaluation of remediation degree and degradation status of the contaminants.

Within the TRansparent Underground Structures research project (TRUST), we investigate the Direct Current resistivity and time-domain Induced Polarization (DCIP) tomography method and its use within the context of DNAPL contaminated sites (see Johansson et al., 2015). DCIP is a non-invasive and non-destructive geoelectric measurement method that among other things has high potential for providing indirect evidence of contaminant degradation status. It is an emerging and promising technique for 2D, 3D and 4D mapping of underground hydrogeochemical structures. Examples of application areas are landfill characterization (*e.g.* Gazoty et al., 2012a, 2012b; Leroux et al., 2007; Cardarelli and Bernabini, 1997), spatial and temporal distribution of contaminants such as ions pollutants leaching from landfill sites (*e.g.* Dahlin et al., 2010; Acworth and Jorstad, 2006; Chambers et al., 2006; Dahlin et al., 2002) and characterization of DNAPL polluted sites (*e.g.* Cardarelli and Di Filippo, 2009; Deceuster and Kaufmann, 2012; Orozco et al., 2012; Power et al., 2014). Furthermore, gas migration within landfills (e.g Rosqvist et al., 2011), and underground CO_2 migration (Auken et al., 2014) including chemical changes resulting therefrom (Doetsch et al., 2015) have been monitored with DCIP.

In this study we have investigated a highly polluted old industrial (textile and mechanical industry) area, contaminated with trichloroethene (TCE) and 1,1,1-trichloroethane (TCA), both DNAPLs, as well as its degradation products and cyanide, chromium, zinc and cadmium (Tornberg et al., 2008). At the investigated site, a small pilot test has been carried out for remediation of the DNAPLs by stimulated reductive dechlorination. DNAPLs are specifically problematic pollutants to delineate with conventional methods due to their dense properties and ability to move independent of the groundwater flow direction, their harmfulness and, risks for unforeseen spreading when drilling and pumping. The fact that chlorinated solvents have been used in almost every little village's dry cleaning facilities means that the pollutant situation is far from unique, and it is highly important to develop better investigation tools, remediation research and cheap non-invasive monitoring techniques.

The aim of this study was to investigate possible uses, benefits and limitations of the DCIP technique divided into the following research questions;

1. Understanding of the underground system;
   Can we improve the understanding of the hydrogeological system (water conditions, pollutant situation, soil conditions, bedrock quality and tectonic structures) by DCIP measurement studies?
2. Understanding of the pollutant situation;
   Can we delineate chlorinated solvents source areas, *i.e.* does DCIP signals correlate to free phase pollutant concentrations measured in groundwater samples?
   Can we delineate pollution plumes associated with TCE pollutants, *i.e.* does DCIP signals correlate to concentrations of TCE and its metabolites in groundwater samples?
   Can we identify an area where *in-situ* remediation test is carried out by carbon source injection, *i.e.* does DCIP signals correlate to the area?
3. Time lapse measurements; Is it possible to monitor changes within a stimulated *in situ* remediation test area, in time steps, and thereby visualize degradation and bioactivity through time, *i.e.* can changes in the area be seen in repeated DCIP measurements and verified by enhanced biological activity?

2. Background and study area

The study area located in Varberg, southwest Sweden, has a history of polluting activities starting in the late 19th century with textile manufacturing using Cr, Zn and Cd for >60 years. The business then turned into precision mechanics with surface finishing of metals and use of zinc, chromium, cyanide and chlorinated solvents (TCE and TCA). The chlorinated solvents are the most problematic contaminants at the site with levels in groundwater of >20 mg/L of TCE and/or its metabolites. Except for handling of chemicals within the manufacturing processes, the pollutants have been spread *via* a leaky wastewater drain pipe, into a concrete sedimentation basin used for treatment of wastewater, and is now refilled with rubble, concrete and soil (Tornberg et al., 2008; Larsson and Hübinette, 2003).

A new railroad tunnel beneath the city is planned in the groundwater flow direction from the site, and the pollution problem has become critical to deal with, as lowering of the groundwater table during the construction will increase the groundwater flow gradient and faster transport of pollutants will occur.

The site outline is presented within Fig. 1 with a sketch of the general groundwater flow towards the sea in W and SW, extent of known bedrock fratures, the contaminant plume delineated from traditional investigations such as drillings, probe soundings and groundwater wells sampled, all performed before our measurements started in 2014 and forming the background baseline for our measurements. Geological profiles are shown in Fig. 2.

Varberg is located below highest shoreline with dominating sediments of postglacial sands and wave-washed gravel (Påsse, 1990). At the site the sandy sediments are overlain by fill, consisting of soil, brick and concrete pieces. The thickness of sediments at the site varies between 2.7 and 5.3 m (Magnusson and Samuelsson, 2004, see Fig. 2). The sediment thickness increases westwards from the site towards the harbour with up to *c.* 18 m of quaternary sediments, and fine grained sediments such as clays interfinger the sandy sediments and divides the gravelly aquifer in two parts (Hübinette and Bank, 2011). Underneath the sediments, dominating bedrock is granodiorite, patches of gneissic banded granite and charnockite. Exposed bedrock north of the site shows five dominating orientations of fractures and lineaments 1) NW, 2) NNW, 3) N, 4) NE and 5) E (SGU, 2006). The fracture system creates a zigzag transport pattern within the bedrock and allows for downwards movement of the DNAPL pollutants. Both ground and bedrock surfaces are dipping westwards (Fig. 2b) with a low point in the bedrock in the central part of the site (Fig. 2a) (Tornberg et al., 2008).

The fill, sandy sediments and fractured bedrock together form a heterogeneous unconfined aquifer. These highly permeable sediments and the bedrock fracture system provide fast transport pathways. Estimates of hydraulic conductivity by test pumping and slug tests show values in the order of 10^{-5}–10^{-8} m/s (Florén, 2015; Davidsson, 2013) Precipitation in Varberg is about 870 mm/year (SMHI, 2013) and evapotranspiration is estimated to >550 mm (Karlqvist et al., 1985). Runoff is calculated to be 300 mm (Karlqvist et al., 1985), which estimates the net infiltration to the aquifer to <20 mm per year.

In January 2013 a pilot study for *in situ* remediation by injection of electron donor and carbon source, HRC Primer® (glycerol tripolylactate, glycerine and lactic acid) and 3DMe® (water, neutralized fatty acids, glycerol tripolylactate and Hydrogen Release Compound Partitioning Electron Donor (Regenesis, US Patent 7667062 B2)), was performed to stimulate already existing bacteria in the subsurface to perform reductive dechlorination by anaerobic degradation. The injected stimulus is described as a long-term controlled release of lactic, organic and fatty

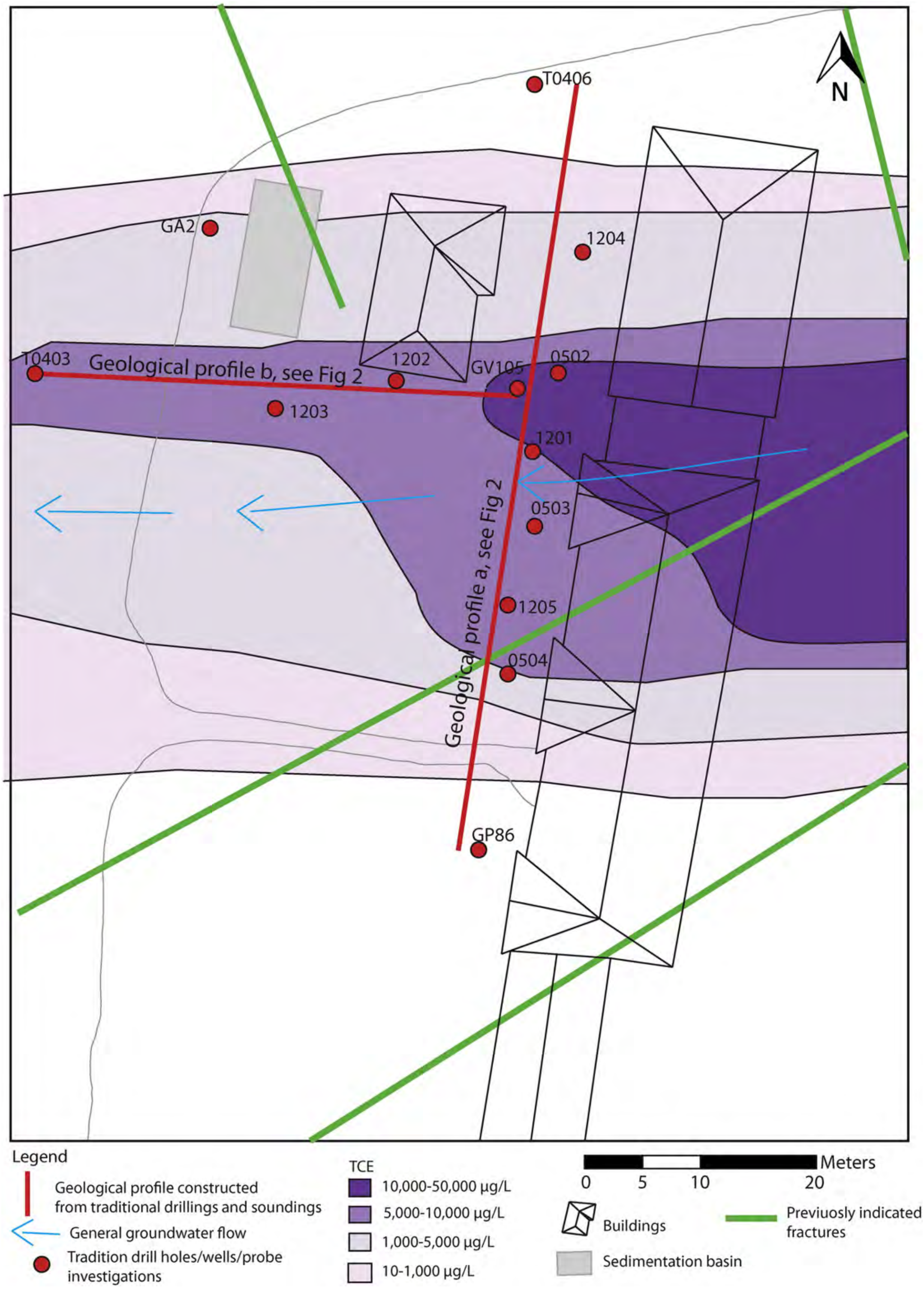

Fig. 1. A sketch of the site and summary of the contaminant delineation results from earlier traditional drill holes/wells/probe investigations presented by Tornberg et al. (2008), Magnusson and Samuelsson (2004) and Davidsson (2013), as well as the general groundwater flow taken from Tornberg et al. (2008). Previously known fractures are taken from Hubinette and Bank (2011). Location for geological profiles presented in Fig. 2 are also shown, as well as location of earlier drill holes/wells/probe investigations used for the construction of the profiles.

acids for the production of hydrogen and electrons for enhanced anaerobic biodegradation (Regenesis, 2016). Carbon source injection of 4410 L in total of the mix was performed by direct push in 8 points (Fig. 3) down to *c*. 5 m within the TCE plume (Hinrichsen et al., 2013). The *in situ* remediation and degradation was followed by sampling and analyses of Dehalobacteria and Dehalococcoides within wells 1201, 0502 and GV105, with analyses and verification of the presence of the BAV1 functional gene and increased microbial activity for the monitored 4.5 months with up to 400 times as many Dehalococcoides (Davidsson, 2013). The largest microbial activity was shown in well 1201, where yet another functional gene was found (tceA reductase) (Davidsson, 2013) indicating degradation from TCE to dichloroethene (DCE) and pointing towards a possible complete degradation via DCE, vinyl chloride (VC) into ethane. The occurrence of DCE and VC also

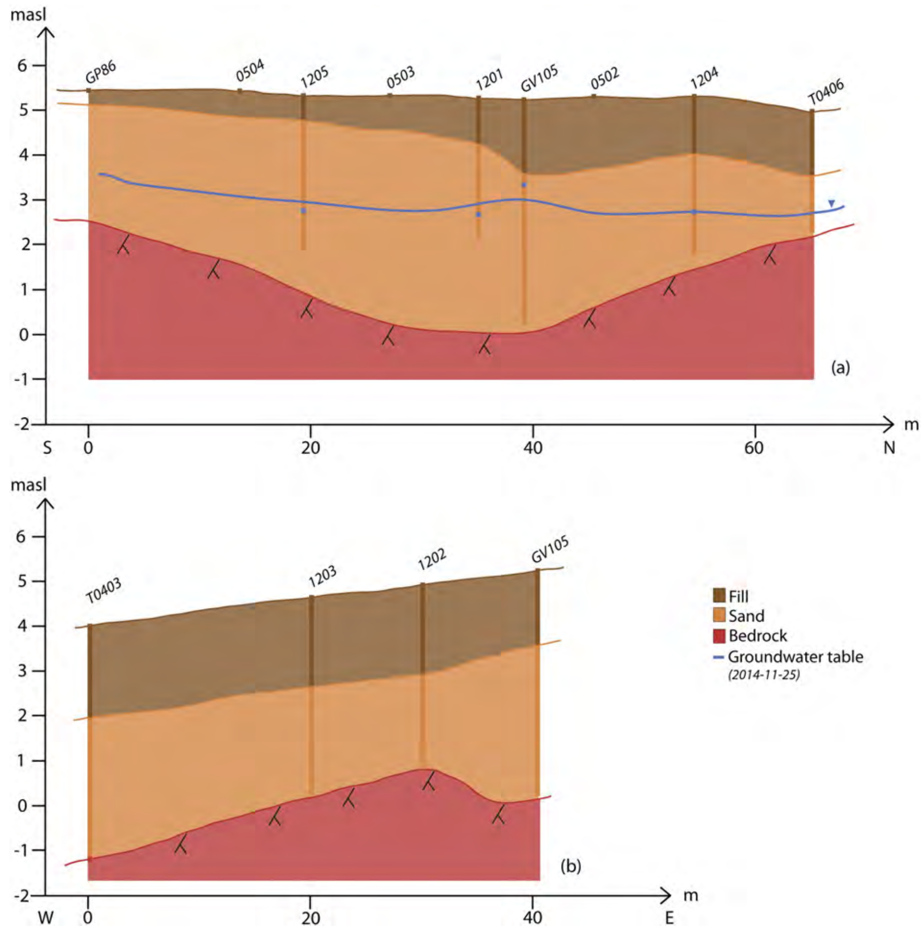

Fig. 2. Geological soil profiles of the site (data from Magnusson and Samuelsson (2004), Tornberg et al. (2008) and Davidsson (2013). Profile a) is drawn from S to N and b) from W to E. Installed monitoring wells are indicated with well number and the orange line corresponds to the casing. For geographic orientation of wells and profiles, see Fig. 1. Modified with permission from Åkesson (2015).

increased some months after the carbon source injection (Davidsson, 2013).

3. Methodology

The methods used for this investigation is a combination of steps and methods as follows; 1) Electromagnetic metal detector and magnetic gradient, 2) DCIP measurements, and 3) Groundwater measurements, sampling and analyses.

3.1. Electromagnetic metal detector and magnetic gradient

Electromagnetic metal detector and magnetic gradient investigations were performed to identify the possible existence of objects causing responses in DCIP, *i.e.* metal reinforcements, cables, drainage pipes and alike. The transient electromagnetic (EM) response was measured with a Geonics EM61 and magnetic gradient with Geometrics G-858 MagMapper. The measurements were performed in three areas as shown in Fig. 3.

3.2. DCIP

Seven DCIP profiles were measured once or more, at three different times (20-21st of May 2014, 25-26th of November 2014 and 17th of February 2015). An ABEM Terrameter LS and an ES10-64C external relay switch were employed together in order to use separated cable spreads to enhance IP data quality as suggested by Dahlin and Leroux (2012). Two parallel electrode cable layouts with 41 electrodes each shifted half a step relative to each other gave a total layout of 82 electrodes with an electrode spacing of one meter (Fig. 3). Stainless steel electrodes were used throughout and positions of electrodes as well as the topography were measured with a Topcon GR3 differential GNSS equipment. If the pre-measurement check indicated poor electrode contact, additional electrodes were added to increase the contact surface.

A multiple gradient array (Dahlin and Zhou, 2006) protocol with 1603 data points was used for the data acquisition, where one measured line has less data points due to inadequate space for a full spread. The chargeability (IP data) was measured using current transmission on-off time of 2 s in May and February, with 20 milliseconds delay after current turn-off and 1860 milliseconds integration time for the chargeability. During November measurements 1 second current transmission on-off time was used, which led to non-comparable chargeability (Olsson et al., 2015) for November data and thus only the resistivity data presented for those data sets.

Quality control of the measurement data was done using visual inspections tools in the form of pseudosection and multi profile plotting to identify outliers, which resulted in limited data culling. Topography data were added to the data files, even though the difference in topography is small. The data were inverted with the program Res2dinvx32 version: 3.71.115 (Geotomo Software, 2014). A robust (L1-norm) inversion constrain was used to allow for large contrasts in the data and models (Loke et al., 2003). Time lapse inversion (Dahlin and Loke,

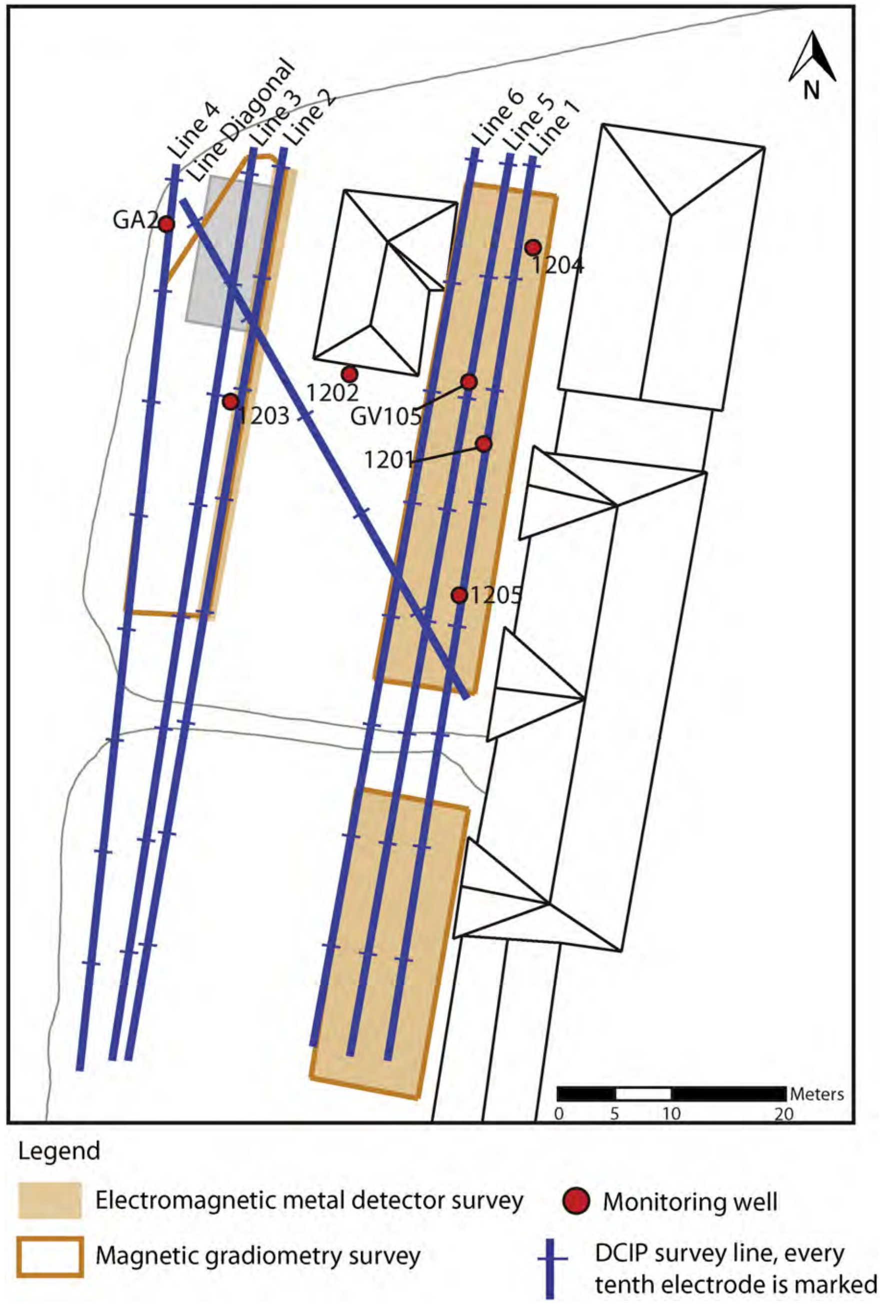

Fig. 3. Surveyed DCIP-lines are shown in blue, areas for electromagnetic measurements shaded in orange, magnetic measurements delineated with orange lines, sampled groundwater wells in red circles and injections points in green circles. The position of the sedimentation basin is shown as a grey rectangle in NW. Houses marked with black lines and roads and paths marked with grey lines. Modified with permission from Åkesson, 2015.

2015) was made for Line 1, with data sets recorded in May 2014 and February 2015, using Res2dinvx64 version 4.05.09.

3.3. Groundwater sampling

Water samples were taken in seven wells (Fig. 3) the 26th of November 2014, after recovering from purging three well volumes with an Eijkelkamp peristaltic pump (12 V). The groundwater was investigated in field with an Aquareader flowcell AP-800 Aquaprobe® and in accredited laboratory. Parameters measured in field were: temperature, oxidation-reduction potential, pH, electrical conductivity, total dissolved solids, salinity and turbidity. Collected samples were kept cold until delivered to the laboratory the next day. The samples were analysed for metals, dissolved organic carbons (DOC), total organic carbons (TOC), chlorinated solvents (1,1-dichloroethane, 1,2-dichloroethane, dichloro-methane, *trans*-1,2-dichloroethene, *cis*-1,2-dichloroethene, 1,1,1-trichloroethane, 1,1,2-trichloroethane, tetrachloroethene, tetrachloromethane, trichlorothene trichloromethane, monochlorobenzene, dichlorobenzenes, 1,2-dichloropropane, 1,1-dichloroethene and vinyl chloride), and chloride.

4. Results and interpretation

4.1. Electromagnetic (EM) metal detection

Results from the EM survey show seven anomalies divided among the three survey areas (Fig. 4a). Three anomalies marked A are visible in Survey area I and correlate to reinforced concrete in the sedimentation basin. Three anomalies marked B in Survey area II correlates with metal well lids. No infrastructural explanation has been found for the C anomaly in Survey area III, but it is possible that it represent a cable or a leaky pipe that is not marked in official infrastructure records.

4.2. Magnetometry

Results from the magnetic gradient measurements (Fig. 4b) show anomalies marked A in Survey area I, which correspond to the concrete reinforcement within the sedimentation basin. Anomalies marked B are interferences from the neighbouring buildings and two anomalies marked C in Survey area II, can be correlated to a waste water pipe and an electric cable. Anomaly D, furthest south in Survey area III is so far unexplained from our review of all available infrastructural documentation, but anomaly E correlates to anomaly C in the EM measurements (Fig. 4a), which is interpreted as a probable leaky pipe, but infrastructural documentation is lacking.

4.3. Groundwater samples

Results from measured and analysed groundwater parameters are shown in Table 1. Note the negative oxidation-reduction potential in all sampled wells. The well closest to the sedimentation basin (GA2) has the highest levels of all contaminants, except for vinyl chloride and zinc. Levels of TCE, 1,1,1-TCA, *cis*-1,2-DCE and *trans*-1,2-DCE are very high and indicates possible free-phase, at least for TCE and *cis*-DCE, where free-phase can be assumed where concentrations are >14,000 μg/L (Swedish Geotechnical Society, 2011; Pankow & Cherry 1996).

TCE levels between 58 and 20,000 μg/L are found in five of the wells; 1201, 1204, 1205 GV105 and GA2, and levels are much higher than the national guideline value of 10 μg/L (SGU, 2013) for TCE and PCE together in groundwater.

4.4. Direct current resistivity

An overview of inverted resistivity sections show two major continuous low resistivity anomalous zones (black lines, Fig. 5) that extends through the area. The broader northernmost continuous anomaly (also Fig. 6, zone 4) is interpreted as a fracture zone within the bedrock, partly water bearing, and probably a major groundwater pathway in the bedrock. This interpretation is supported by previous core investigations by Döse (pers. com. June 2015, Christin Döse, Tyréns AB). The decrease in resistivity in this zone can be a result of higher groundwater content and/or transport of degradation products of TCE and TCA. Chloride ions are released in each degradation step leading to increased electrical conductivity in the groundwater and possibly affecting and lowering the IP responses in the fracture system/soil pores. The fracture zone seems to have a good connection and/or, the same pollutant situation as the soil cover within the bedrock depression to the southeast (shown as the “bent” dashed black line in Fig. 5) and hence giving the same low resistivity values.

In general, the profiles can be divided into three layers or zones; 1) the uppermost high resistivity zone about three meters thick, corresponding to unsaturated soil cover (Fig. 6, zone 1). Below, with lower resistivity values is the saturated zone consisting of the sandy soil and part of the uppermost fractured bedrock (Fig. 6, zone 2). The third zone is high resistive and consists of non to little fractured “high quality” bedrock (Fig. 6, zone 3). The layer interpretation is supported by available drill logs (see Fig. 2).

In the fence diagram, two other anomalous areas, one low resistive (Fig. 6, zone 5) and one high resistive (Fig. 6, zone 6), are marked in the north part of Line 2 and 3 (Fig. 5). Zone 5 is interpreted as the rubble filled sedimentation basin and zone 6 could be either a 3D effect of the terrace construction beside or the sedimentation basin, and/or a larger boulder or part of a bedrock outcrop. Due to edge effects and poor constraints, we are not inclined to draw any more conclusions from that anomaly. The low resistivity area downstream from the sedimentation basin (Fig. 5), we interpret as a result of high concentrations of pollutants and metabolites possibly accumulating due to leakage, runoff and/or infiltration from the sedimentation basin area, also indicated by the high electrical conductivity in well GA2, at 466 μS/cm (see Table 1 for results of concentrations and groundwater parameter measurements), showing the highest values of all sampled wells. It could also be a result of the direct push test in 2013, where the injected carbon source has pushed TCE, metabolites and metal ions (Cr and Zn)

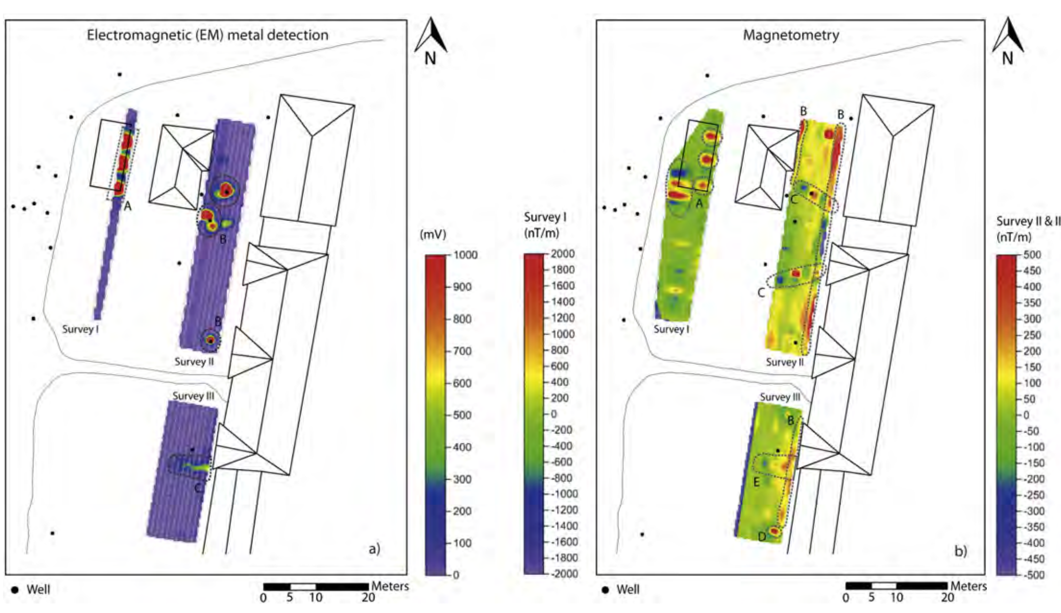

Fig. 4. a) Results from the EM survey. Anomaly A (Survey area I) corresponds to concrete reinforcement in the sedimentation basin, anomaly B (Survey area II) corresponds to metal well lids, and anomaly C (Survey area III) is interpreted as a leak of something yet unidentified. b) Results from the magnetometry survey. Anomalies A represent concrete reinforcement in the sedimentation basin and B-anomalies are interpreted as magnetic effects from the neighbouring buildings. The C anomalies (Survey area II) are interpreted as electricity cables. For anomaly D, no corresponding infrastructure have been found from maps and anomaly E, correlates to anomaly C in the EM measurements (see a)) and a probable leaky pipe. Note that due to large variation in magnetometry values between Survey area I (scale to the left) and Survey areas II-III (scale to the right in the map), different scales are used in the figure. Houses and roads are marked with black lines.

Table 1
Groundwater chemistry data analysed and on-site measured parameters. Values in bold mark concentrations above guideline values.

Well analysed	Unit	1201	1202	1203	1204	1205	GV105	GA2	Guideline values
TCE	μg/L	**1100**	6,9	3,2	**58**	**510**	**300**	**20,000**	10[a]
1,1,1-TCA	μg/L	430	43	29	1,5	<1.0	290	1500	
1,1-DCE	μg/L	55	16	10	0,86	9,6	50	120	
cis-1,2-DCE	μg/L	5800	1700	1100	67	370	5100	21,000	
trans-1,2-DCE	μg/L	100	44	14	3	7.8	220	1000	
1,1-DCA	μg/L	180	360	240	3	47	430	610	
VC	μg/L	**200**	**2100**	**1200**	**1**	**3**	**2100**	**460**	0.50[b]
Cl	μg/L	52	42	56	45	33	51	82	100[b]
DOC[c]	mg/L	12	16	16	6.7	5.1	18	9.5	
TOC[d]	mg/L	13	16	19	6.9	6.6	21	9.5	
Cadmium	μg/L	0.035	0.016	0.011	0.021	0.015	0.010	0.016	5[b]
Chrome	μg/L	**1.9**	**3.1**	**3.1**	**1.0**	0.72	**2.1**	**6.1**	1[a]
Zinc	μg/L	9.9	2.4	2.0	4.7	1.3	1.2	65	100[a]
Iron	mg/L	**0.53**	**5.7**	**3.1**	**0.18**	**0.1**	**1.7**	**1.2**	0.100[b]
Manganese	mg/L	**0.07**	**0.26**	**0.13**	<0.03	0.03	**0.18**	**0.56**	0.050[b]
Measured									
Temperature	°C	12.7	11.7	11.9	11.9	13.6	12.6	11.5	
ORP[e]	mV	−69.1	−86	−6.6	−16.8	−54.5	−24.2	−33.4	
pH		6.65	6.97	7.04	6.84	7.64	6.58	7.02	
Electrical conductivity	μS/cm	**459**	**372**	**395**	**450**	**413**	**414**	**466**	38[a]
Total dissolved solids	mg/L	298	239	266	291	262	265	304	
Salinity	ppt	0.23	0.18	0.19	0.22	0.19	0.20	0.23	
Turbidity	NTU	**31.5**	**10.9**	**180**	**41**	**130**	**27.5**	**17.7**	0.5[b]

[a] SGU (2013) guideline values for groundwater.
[b] SLV (2001) guideline values for drinking water.
[c] Dissolved organic carbon.
[d] Total organic carbon.
[e] Oxidation-reduction potential.

downstream. There are no indications, however, that this is the case as the TOC concentrations in the area is not elevated, which would be the case if carbon source was pushed into the area.

The southernmost continuous low resistivity anomaly (Fig. 5 as a black line; Fig. 6 marked with an x) corresponds to the line of lamp posts along the walking path and is interpreted as a cable trench. The

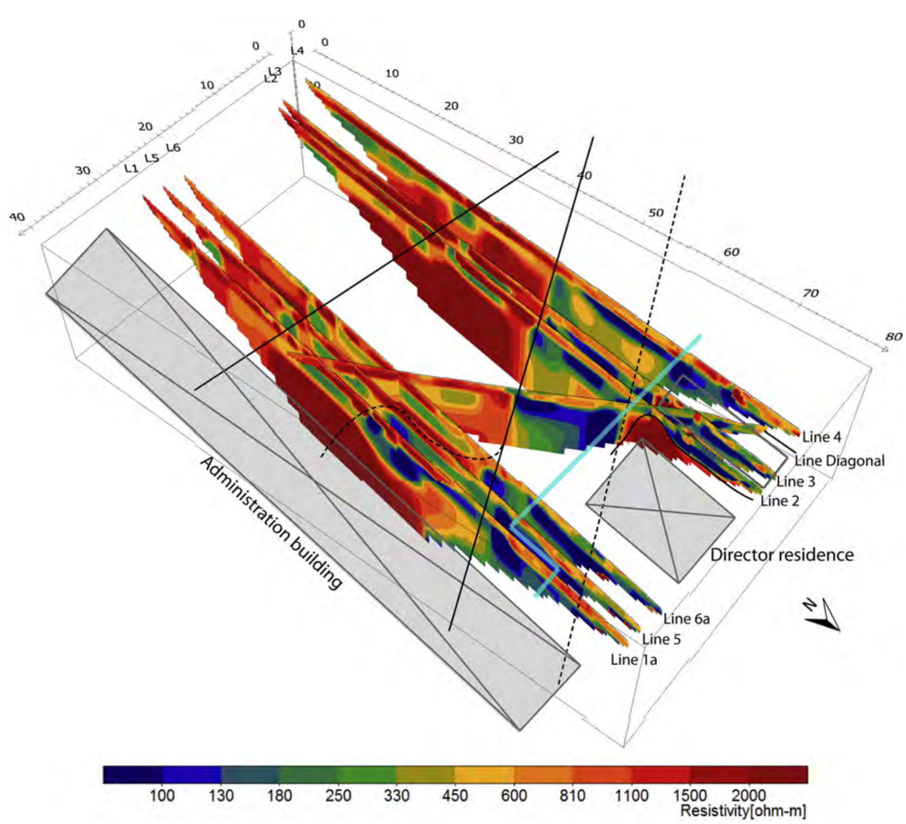

Fig. 5. Resistivity sections joined in a fence diagram. Identified anomalies are marked with black straight for distinct anomaly and dotted lines for a gradual anomaly transition. Houses are marked as grey filled rectangles, the sedimentation basin is marked with a grey non-filled rectangle and the wastewater drain pipe is turquoise. Note the north direction towards the right in the figure, this to be able to show the anomalies as clearly as possible.

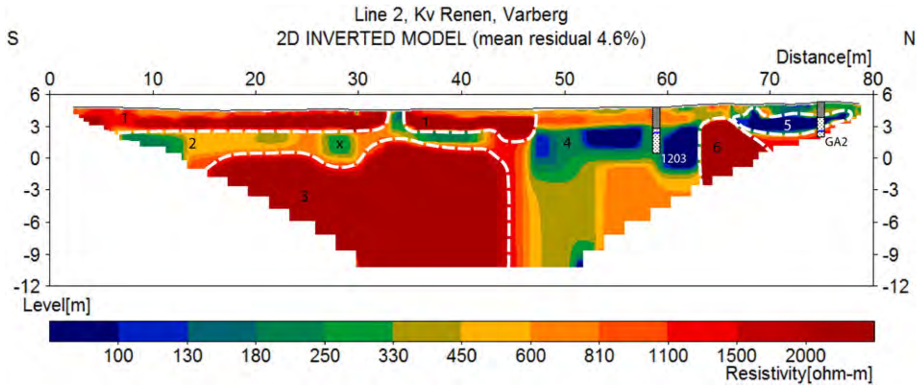

Fig. 6. Resistivity section of Line 2, with three main layers are marked; 1) high resistivity (>450 Ω m) within the unsaturated soil layers, 2) low resistivity (<800 Ω m) corresponding to saturated soil and fractured bedrock and 3) high resistivity (>1100 Ω m) in the non-fractured good quality bedrock. At approximately 45 m into the profile, unit 3 disappears. The area marked 4 with low resistivity values (<800 Ω m) is interpreted as a larger water bearing fracture zone shown as an almost continuous anomaly in Fig. 5. The anomaly marked x corresponds to the line of lamp posts and is interpreted as a cable trench giving low resistivity. The two groundwater monitoring wells are shown with drill logs within the profile (grey = fill material; grey dotted on white = sand; blue line = groundwater level in Nov 2014).

low resistivity could be a result of de-icing salt applied on and infiltrated on the walking path containing fill material with higher hydraulic conductive, leading possible solutes more easily than neighbouring material. Possibly pipes or cables in the trench could also be the origin of the anomalous zone. Other single low resistivity anomalies that can be seen in the 2nd layer (Fig. 6) are probably coarser fill material or macro pore flow channels.

4.5. Induced polarization (IP)

The IP results from May 2014 are shown as a fence diagram (Fig. 7). Black lines encircle high chargeability anomalies (a, b and c in red above 20 mV/V, however b has values >60 mV/V, Fig. 7), which can be identified in three of the four shown sections. Also the lack of high IP-responses are important to note in Line 4.

The IP anomaly marked a (Fig. 7), could possibly be correlated with anomaly C from the EM61 measurements (Fig. 4a) and E from the magnetometry measurements (Fig. 4b). Subsurface objects causing high chargeability marked b (Fig. 7), have been ruled out by the additional geophysical measurements (EM61 and magnetic gradient). Possible 3D effects from the nearby building cannot be ruled out, but since the IP effects only appear at a limited section along the building, it is less likely that the anomaly is solely caused by 3D effects. The source of the IP anomaly b (Fig. 7) is uncertain, but one possible explanation could be a clay weathering zone in connection to the fracture zone identified in the resistivity data. However, the location of the anomaly is also corresponding to the area of electron donor/carbon source injection. In order to evaluate if the electron donor/carbon source injection could cause increased IP effects, a time lapse inversion was performed on data measured in May 2014 and February 2015 respectively. If the anomaly is caused by the injection, changes should be visible as the

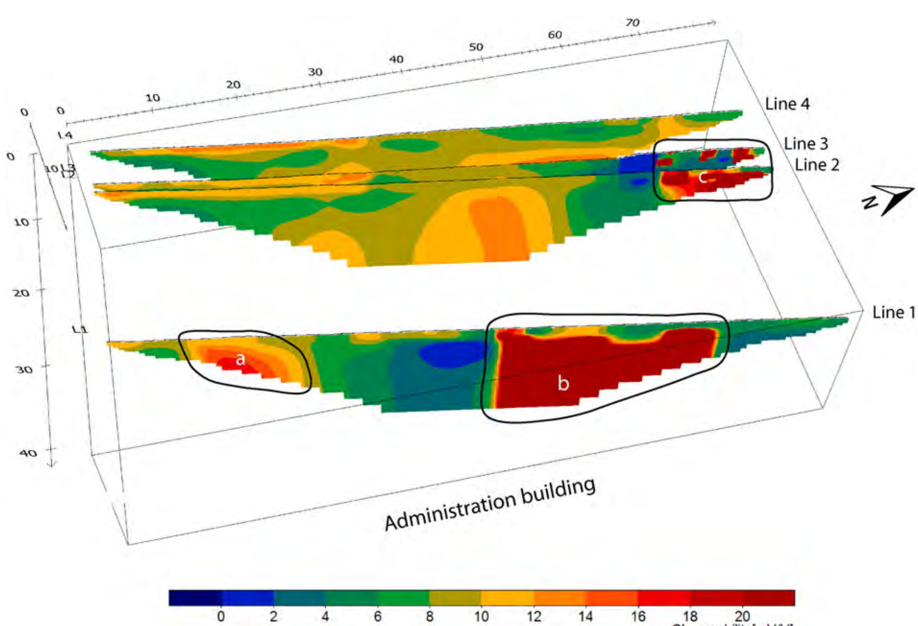

Fig. 7. IP sections measured in May 2014, Line 1, 2, 3 and 4 (see Fig. 3). The area of higher chargeability marked a, corresponds to the yet unexplained anomaly within the EM (C) and magnetometry (E) measurements. The anomaly marked b is interpreted as the injection area. Anomaly c with higher chargeability in Lines 2 and 3 is interpreted to be the reinforced concrete.

carbon source is degraded, whereas if clay weathering is the cause, no quick changes are anticipated. The IP anomaly marked c, correspond to the sedimentation basin area, and are interpreted to be an effect of metal reinforced concrete.

4.6. Time lapse evaluation of DCIP data

Results from Line 1 measured in both May 2014 and Feb. 2015 gives similar IP response, but changes in time are visible (Fig. 8a). An increase in IP response is seen at *c.* 42 m and 50–55 m (α and ɣ, Fig. 8a). The ɣ area (Fig. 8a) is interpreted to be caused by the biogeochemical changes initiated by the carbon source injection and/or be a physical response to the direct push injection decreasing the contaminant concentration by pushing it some distance within the soil and/or causing dissolution. This has possibly led to a difference in pore configuration of the contaminants and a changed IP signal as has been proposed by *e.g.* Johansson et al. (2015). The reason for the IP increase within area α is unknown, but no relationship can be seen to the injection of carbon source. The decrease in IP response at distances 44 and 60 m (β and δ, Fig. 8a) might be interpreted as a response to the either removal of microbes and/or, increase of degradation metabolites or loss of contaminants through either degradation or transport away from the remediation area. From the time lapse analyses, it appears that the center of the injected area increase in chargeability, while the edges of the stimulated area decrease in chargeability.

The changes in resistivity are limited to the upper subsurface part of the section (Fig. 8b). The increase in resistivity in the upper meter could be caused by a decrease in temperature or water content between May and February, or a combination of these. The distinct decrease in resistivity at a couple of meters depth, 28-30 m into the profile, is potentially caused by a leaky pipe or a French drain transporting more de-icing salt ions in February than in May. This anomaly is also indicated in the EM 65 survey results (anomaly C, Fig. 4a). A plausible explanation of the negative anomaly around 40 m is not yet found.

4.7. Comprehensive interpretation

By combining resistivity and IP measurements with data from traditional investigation techniques, (groundwater analysis, drill logs, geotechnical and geological investigations), a detailed geologic and hydrogeological model could be made for remediation test site (Fig. 9). The bedrock can be interpreted as constituted of high quality areas and low quality areas, the latter corresponding to the SW-NE directed fracture zone recognized by resistivity measurements (Figs. 5 and 6). Investigations nearby confirms a water bearing fracture zone to the southwest with strike and dip: 250°/45° (personal communication, C. Döse June 2015).

As the increase in IP-signal can be explained by geochemical changes, temperature changes and/or microbiological activity, the purple area in Fig. 9, with higher chargeability at *c.* 50–53 m, is interpreted as a zone with increased chemical and/or biochemical activity due to the injected stimulus. This is coherent with Davidsson (2013) earlier reported high microbial activities (Dehalococcoides) in well 1201 and a more complete degradation in this area. The higher activity within this zone is possibly an effect of the bedrock depression retaining the electron donor/carbon source, leading to an enhanced stimulated reduction process as planned and indicated by the microbial analyses (Davidsson, 2013) and higher TCE levels than in the wells located within the fracture zone. The process and cause of the IP-signal increase is uncertain and more comprehensive studies are needed for detailed understanding and confirmation. The decrease in IP-signal at 60 m could be caused by drainage of pollutants, electron donor/carbon source and microbes from the area, due to higher hydraulic conductivity within the fracture zone. This is also agrees well with the lower levels of TCE (Table 1) and microbial degradation activity (Davidsson, 2013) in wells within the fracture zone area. The fracture zone is possibly a highly potent transport pathway for pollutants, injected stimulus and microbes out from the estate towards the south-west. The other area of decrease in IP-signal at *c.* 44 m is interpreted as a loss of TCE and an increase of degradation metabolites, also possibly a decrease in microbes due to a

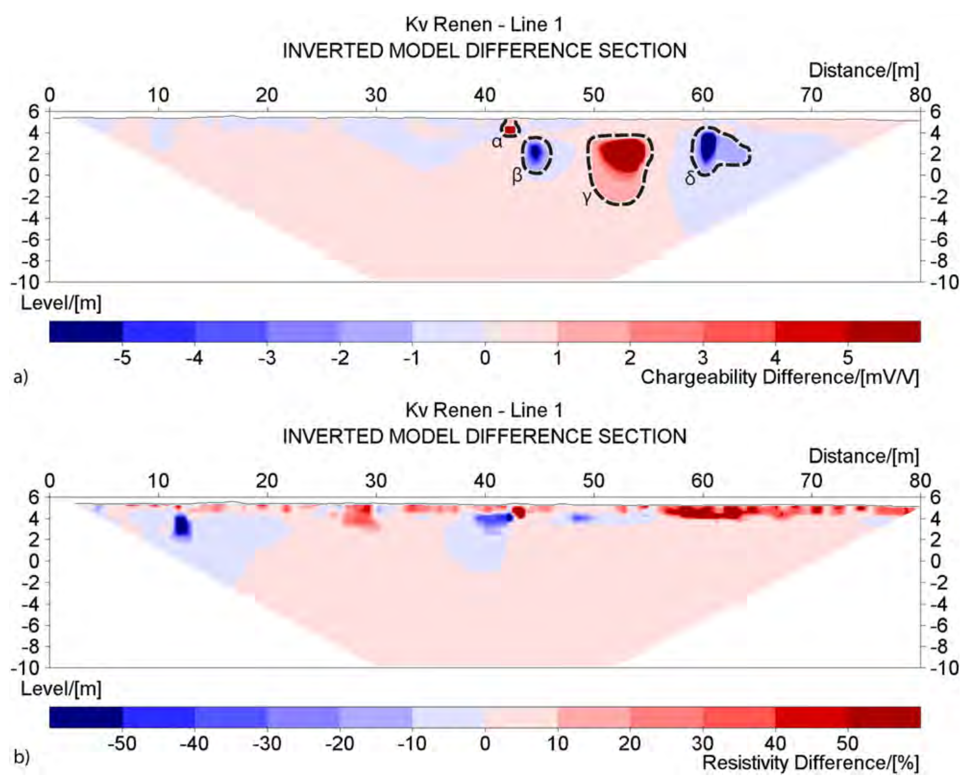

Fig. 8. Time lapse sections for Line 1 (location, see Fig. 3) measured in May 2014 and February 2015 a) differences in IP-signal sand b) differences in resistivity measured.

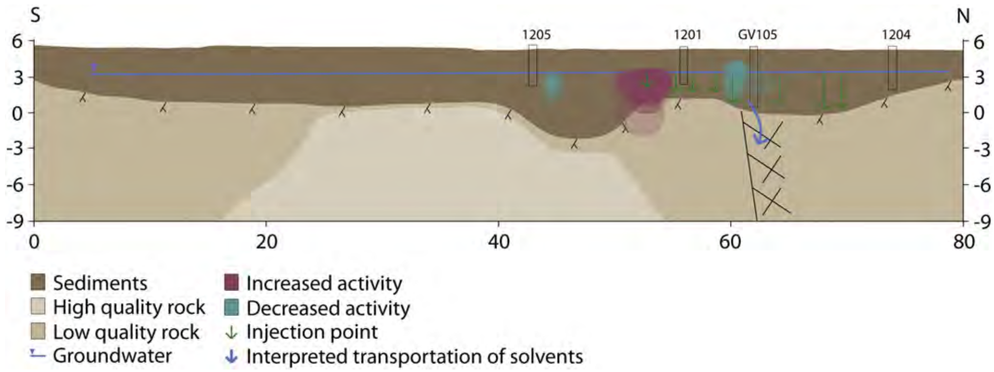

Fig. 9. A detailed geo/environmental model from Line 1 based on resistivity data and the time lapse studies of resistivity and IP-signals, groundwater chemistry and -levels, drill logs and geotechnical and geological investigations in the area. After 60 m, a fracture zone appear, which could explain the decrease in IP-signal as both pollutants, injected stimulus and possibly active microbes easily can be transported from the area within the highly hydraulic conductive zone. At around 50 m, activity increases from May 2014 to February 2016 and could possibly be explained by the bedrock surface depression retaining both the pollutants and the injected carbon source where microbes possibly are active degrading both the stimuli and the chlorinated hydrocarbons. The decrease around 45 m could be either an "edge effect" where metabolites increase as TCE decrease due to degradation, or injected stimulus moving through the sand soil.

decrease in injected stimulus in the edge area. Another possible explanation could be movement of the stimulus through the sandy soil.

5. Discussion

In brownfield areas, the most common investigation techniques are digging, drilling, and well screen installations for sampling. These techniques are all used to find, delineate and monitor changes within the pollutant situation and at a later stage, to verify the effect of remediation efforts. Biogeochemical changes within the subsurface cause changes in geophysical properties and hence give rise to different DCIP responses.

From investigations with DC resistivity, we can achieve an almost continuous picture of the underground structures with differences in rock quality, soil cover, groundwater surface level and aquifer geometry, as has been discussed and shown in several studies before (*e.g.* Dahlin, 1996; Dahlin et al., 1999; Binley and Kemna, 2005; Danielsen et al., 2007). From previous drill references in the area, we can confirm our interpretations of the geological setting and, we were also able to find other previously not identified structures at the site, such as the larger water bearing fracture zone marked in Figs. 5 and 6. Even though numerous drillings had been performed previously, none had been placed within this fracture zone and hence, this major groundwater transport pathway was not taken into consideration when pollution transport was investigated and calculated prior to our investigation. However, to be able to verify interpreted geological settings from DC resistivity, drillings are needed. If geoelectric investigations are performed at an early stage of the site investigation, drilling location can be carefully chosen from the inverted DC resistivity sections to verify zones interpreted as anomalies and geological structures, hence a more reasonable selection of drilling sites could be done. The DC resistivity results would have helped minimize the number of boreholes and maximized the information withdrawn from the more invasive investigation techniques, and hence possibly minimized investigation costs.

The DC resistivity time lapse mostly indicates changes in the upper one to two meters and is possibly attributed to changes in water content and soil temperature.

From the IP measurements we retrieved spatial distribution indications of the pollutant and/or injected electron donor/carbon source stimulus. We can from the high IP signals pinpoint the area where stimulus have been injected into the TCE source area. The reason for the high chargeability signals could be attributed to different processes, mainly; 1) enhanced microbial activity (*e.g.* Abdel Aal et al., 2006; Atekwana and Slater, 2009), 2) increased degradation of TCE resulting in residual free phase contaminant droplets possibly trapped within the pore system (see Johansson et al., 2015). The same effect as degradation of TCE can be expected when the injected carbon source, that provides 3DMe® emulsion micelles, get trapped within the pore system (see Johansson et al., 2015). More research on the processes and cause of IP signal increase is needed to verify or discard either of, or the combination of the suggested interpretations.

Changes within the stimulated area through time are visible within the IP time lapse results and are mainly attributed the biogeochemical changes within the area and agree well with the microbial results given by Davidsson (2013). The stimulus can according to the manufacturer be active for up to three years and the large IP anomaly and changes therein are likely to be a result of the stimulus. If this is the case, there are great possibilities to follow and monitor the changes underground for this type of *in situ* remediation with IP measurements. Possibly could other types of *in situ* remediation actions also be monitored by DCIP? More research to test the usefulness of DCIP monitoring on different types of *in situ* remediation actions for chlorinated hydrocarbons, would be highly eligible, as the success of *in situ* remediation is hard to verify by sampling from groundwater alone. The non-invasive and non-destructive character of DCIP investigations is appealing as it reduces the risk of exposure and prevents disturbances to the degradation/chemical reactions in the existing environment by invasive sampling or drilling.

The high IP anomalies shown in the results from the highly polluted sedimentation basin are possibly caused by the reinforced concrete construction, as also indicated by the EM and magnetic results. Perhaps the TCE would give an IP signal as well from this area, would it not be for the reinforcements. The possible IP signals are, however, masked by the reinforcement signals. This shows that IP investigations are not effective when tracing chlorinated hydrocarbons in areas with too many metal objects as, especially surfaces with reinforced concrete.

6. Conclusion

The DCIP investigation method has shown to be highly useful when creating a subsurface model and improve the understanding of the hydrogeological system and changes with time therein. The DC resistivity would be best used in a pre-investigation phase to pinpoint changes within the underground to more wisely choose drilling locations. Drillings and sampling of soil, bedrock and groundwater can then be used to verify the interpreted geological subsurface structure and aquifer geometry. The IP measurements could detect and delineate an area where stimulus for reductive dechlorination had been injected by direct push into a TCE source area. The high IP signals from the stimulus injected area could be due to one of, or a combination of the following processes;

1) Increased chargeability due to enhanced biologically induced biochemical processes.
2) Increased degradation of TCE resulting in trapped residual free phase TCE droplets within the pore system (see Johansson et al., 2015).
3) The injected stimulus is described to provide free charges in the form of hydrogen and electrons which could give rise to changes in groundwater conductivity which in turn could affect the chargeability.

The combined use of DC resistivity and IP can be powerful when delineating the contaminant situation in time and space, as the DC resistivity provides a good image of the geology, hydrogeology and groundwater fluctuations, while the IP results will provide an image of the biogeochemical spatial and temporal changes underground when time lapse investigations are performed. More research to verify the causes of the IP signal changes is, however, needed to be certain of the processes creating the IP signals. For the investigated site, the TCE source areas could not be delineated by DCIP alone, in this case due to subsurface constructions of reinforced concrete and to the injected stimulus, masking the possible low IP response from the TCE constituting a possible electrical insulator. Caution in over interpreting the results should be taken as other underground objects can cause IP responses, and complementary methods like EM and/or magnetometry can be used to verify metal objects, cables or alike to prevent misinterpretations.

The high IP signal and changes through time in the stimulated area give future expectations of possible monitoring approaches with the IP time lapse method in the field of *in situ* remediation actions. This is an area in great need of a non-invasive continuous monitoring approach as the current sampling methodology is inadequate and the possibility needs further exploration.

Conflicts of interest

There is no conflict of interest among the authors.

Acknowledgment

Funding for the work was provided by Formas - The Swedish Research Council for Environment, Agricultural Sciences and Spatial Planning, (ref. 2012-1931), BeFo - Swedish Rock Engineering Research Foundation, (ref. 331), SBUF - The Development Fund of the Swedish Construction Industry, (ref. 12719), SSF - Swedish Foundation for Strategic Research (ref. SM13-0056) and Sven Tyréns Stiftelse. The project is part of the Geoinfra-TRUST framework (http://trust-geoinfra.se/).

Appendix A. Supplementary data

Supplementary data to this article can be found online at http://dx.doi.org/10.1016/j.scitotenv.2016.09.117.

References

Abdel Aal, G.Z., Slater, L.D., Atekwana, E.A., 2006. Induced-polarization measurements on unconsolidated sediments from a site of active hydrocarbon biodegradation. Geophysics 71 (2), H13–H24.
Acworth, R.I., Jorstad, L.B., 2006. Integration of multi-channel piezometry and electrical tomography to better define chemical heterogeneity in a landfill leachate plume within a sand aquifer. J. Contam. Hydrol. 83, 200–220.
Åkesson, S., 2015. The Application of Resistivity and IP-measurements as Investigation Tools at Contaminated Sites: A Case Study From Kv. Renen 13, Varberg, SW Sweden. Master's thesis no 442, Lund University (82 pp).
Atekwana, E.A., Slater, L.D., 2009. Biogeophysics: a new frontier in earth science research. Rev. Geophys. 47 (4), 1–30.
Auken, E., Doetsch, J., Fiandaca, G., Vest Christiansen, A., Gazoty, A., Cahill, A.G., Jakobsen, R., 2014. Imaging subsurfacemigration of dissolved CO_2 in a shallow aquifer using 3-D time-lapse electrical resistivity tomography. J. Appl. Geophys. 101, 31–41.
Binley, A., Kemna, A., 2005. In: Rubin, Y., Hubbard, S. (Eds.), DC Resistivity and Induced Polarization Methods in Hydrogeophysics. Springer, pp. 129–156.
Cardarelli, E., Bernabini, M., 1997. Two case studies of the determination of parameters of urban waste dumps. J. Appl. Geophys. 36, 167–174.
Cardarelli, E., Di Filippo, G., 2009. Electrical resistivity and induced polarization tomography in identifying the plume of chlorinated hydrocarbons in sedimentary formation: a case study in Rho (Milan-Italy). Waste Manag. Res. 27, 595–602.
Chambers, J.E., Kuras, O., Meldrum, P.I., Ogilvy, R.D., Hollands, J., 2006. Electrical resistivity tomography applied to geologic, hydrogeologic, and engineering investigations at a former waste-disposal site. Geophysics 71 (6), B231–B239.
Dahlin, T., 1996. 2D resistivity surveying for environmental and engineering applications. First Break 14 (7), 275–283.
Dahlin, T., Leroux, V., 2012. Improvement in time-domain induced polarisation data quality with multi-electrode systems by separating current and potential cables. Near Surface Geophysics 10, 545–565.
Dahlin, T., Loke, M.H., 2015. Resistivity-IP monitoring at landfills in southern Sweden. Procs. GELMON 2015 (1p).
Dahlin, T., Zhou, B., 2006. Multiple-gradient array measurements for multichannel 2D resistivity imaging. Near Surf. Geophys. 4, 113–123.
Dahlin, T., Bjelm, L., Svensson, C., 1999. Use of electrical imaging in site investigations for a railway tunnel through the Hallandsås Horst. Sweden: Q. J. Eng. Geol. 32, 163–172.
Dahlin, T., Bernstone, C., Loke, M.H., 2002. A 3D resistivity investigation of a contaminated site at Lernacken in Sweden. Geophysics 67 (6), 1692–1700.
Dahlin, T., Rosqvist, H., Leroux, V., 2010. Resistivity-IP for landfill applications. First Break 28 (8), 101–105.
Danielsen, J.E., Dahlin, T., Owen, R., Mangeya, P., Auken, E., 2007. Geophysical and hydrogeologic investigation of groundwater in the Karoo stratigraphic sequence at Sawmills in northern Matabeleland, Zimbabwe: a case history. Hydrogeol. J. 15, 945–960.
Davidsson, L., 2013. Slutredovisning av utförda undersökningar och tester Renen 13 i Varberg. [Unpublished consulting report.]. WSP Environmental, Halmstad (92 pp).
Deceuster, J., Kaufmann, O., 2012. Improving the delineation of hydrocarbon impacted soils and water through induced polarization (IP) tomographies: a field study at an industrial waste land. J. Contam. Hydrol. 136-137, 25–42.
Doetsch, J., Fiandaca, G., Auken, E., Christiansen, A.V., Cahil, A.G.l., Jacobsen, J.D., 2015. Field scale time-domain spectral induced polarization monitoring of geochemical changes induced by injected CO_2 in a shallow aquifer. Geophysics 80 (2), WA113–WA126.
Florén, S., 2015. Grundvattenbildning till berg - En litteraturstudie samt fallstudie av järnvägstunneln delen Varberg-Hamra. Master Thesis in Environmental Sciences. Lund University (68 pp).
Gazoty, A., Fiandaca, G., Pedersen, J., Auken, E., Christiansen, A.V., Pedersen, J.K., 2012a. Application of time domain induced polarization to the mapping of lithotypes in a landfill site. HESS 16, 1793–1804.
Gazoty, A., Fiandaca, G., Pedersen, J., Auken, E., Christiansen, A.V., 2012b. Mapping of landfills using time-domain spectral induced polarization data: the Eskelund case study. Near Surface Geophysics 10 (6), 575–586.
Geotomo Software, 2014. Res2dinv_Guide, RES2DINVx32 ver. 3.71 with multi-core support. Penang, Malaysia. 124 pp. Electronic publication: reachable at: http://www.geotomosoft.com/downloads.php
Hinrichsen, H., Nord, H., Davidsson, L., 2013. Fördjupad åtgärdsutredning, förslag till fortsatta åtgärder. [Unpublished consulting report.] RGS90, Norrköping (140 pp).
Hübinette, P., Bank, A., 2011. Kv Renen i centrala Varberg–Kompletterande miljöteknisk undersökning samt miljö- och hälsoriskbedömning och åtgärdsalternativ med avseende på klorerade lösningsmedel i mark. [Unpublished consulting report.]. Structor Miljö Göteborg AB, Göteborg (201 pp).
Johansson, S., Fiandaca, G., Dahlin, T., 2015. Influence of non-aqueous phase liquid configuration on induced polarization parameters: conceptual models applied to a time-domain field case study. J. Appl. Geophys. 123, 295–309.
Karlqvist, L., De Geer, J., Fogdestam, B., Engqvist, P., 1985. Description and appendices to the hydrogeological map of Halland county. Serie Ah, Nr 8. Geological Survey of Sweden (SGU), Uppsala (73 pp).
Larsson, J., Hübinette, P., 2003. Översiktlig miljöteknisk undersökning av föroreningssituationen i och kring slambassäng, Kv Renen. [Unpublished consulting report.]. Golder Associates AB, Göteborg (40 pp).
Leroux, V., Dahlin, T., Svensson, M., 2007. Dense resistivity and IP profiling for a landfill restoration project at Härlöv, southern Sweden. Waste Manag. Res. 25 (1), 49–60.
Loke, M.H., Acworth, I., Dahlin, T., 2003. A comparison of smooth and blocky inversion methods in 2-D electrical imaging surveys. Explor. Geophys. 34 (3), 182–187.
Magnusson, J., Samuelsson, S., 2004. Kompletterande undersökning av förorening runt slambassäng, Kv Renen 13. [Unpublished consulting report.]. Tyréns, Göteborg (61 pp).
Olsson, P.-I., Fiandaca, G., Dahlin, T., Auken, E., 2015. Impact of time-domain IP pulse length on measured data and inverted models. Procs. Near Surface Geoscience 2015, 6–10 September 2015, Torino, Italy (5 pp).
Orozco, A.F., Kemna, A., Oberdörster, C., Zschornack, L., Leven, C., Dietrich, P., Weiss, H., 2012. Delineation of subsurface hydrocarbon contamination at a former hydrogenation plant using spectral induced polarization imaging. J. Contam. Hydrol. 136–137 (2012), 131–144.
Pankow, J.F., Cherry, J.A., 1996. Dense Chlorinated Solvents and other DNAPLs in Groundwater: History, Behavior, and Remediation. Waterloo Press, Portland, Oregon, Canada (538 pp).
Påsse, T., 1990. Description to the quaternary map Varberg NO. Serie Ae, Nr 102. Geological Survey of Sweden (SGU), Uppsala (117 pp).
Power, C., Gerhard, J.I., Karaoulis, M., Tsourlos, P., Giannopoulos, A., 2014. Evaluating four-dimensional time-lapse electrical resistivity tomography for monitoring DNAPL source zone remediation. J. Contam. Hydrol. 162, 27–46.

Regenesis, 2016. http://regenesis.com/remediation-products/3-d-microemulsion/June2016.
Rosqvist, H., Leroux, V., Dahlin, T., Svensson, M., Lindsjö, M., Månsson, C.-H., Johansson, S., 2011. Mapping landfill gas migration using resistivity monitoring. Waste Resour. Manag. 164 (1), 3–15.
SGU, 2006. Varberg, berggrund och grundvatten vid fastigheten Renen (DNR: 08-443/2006. 7 pp).
SGU, 2013. Bedömningsgrunder för grundvatten. SGU-rapport 2013:01. Sveriges geologiska undersökningar, Uppsala (238 pp).
SLV, 2001. Livsmedelsverkets föreskrifter om dricksvatten, SLVFS 2001:30. Svenska livsmedelsverket/National Food Agency, Sweden (33 pp).
SMHI, 2013. Annual precipitation data, reachable at: http://www.smhi.se/klimatdata/meteorologi/nederbord, read 2014-09-14.
Swedish Geotechnical Society, 2011. Klorerade lös- ningsmedel i mark och grundvatten. Rapport 2:2011. Göteborg, Sweden (42 pp).
Swedish Environmental Protection Agency (SEPA), 2014. Nationell plan För fördelning av statliga bidrag för efterbehandling. Report 6617 (in Swedish). 30 pp).
Tornberg, K., Andersson, J., Falkenberg, J.A., 2008. Markundersökningar och fördjupad riskbedömning på Renen 13, Varberg. [Unpublished consulting report.]. Niras, Stockholm (275 pp).